RSC Advances

PAPER

View Article Online
View Journal | View Issue

Cite this: *RSC Adv.*, 2025, **15**, 23165

Selective production of a jet fuel fraction through hydrocracking of *n*-heptadecane using Pt-supported β-zeolite-Al_2O_3 composite catalysts†

Kosuke Murata,[a] Yugo Nishiura,[a] Shunma Mitsuoka,[a] Mio Horibe,[a] Tadanori Hashimoto,[a] Ning Chen,[b] Yuki Jonoo,[b] Sho Kawabe,[b] Keita Nakao[b] and Atsushi Ishihara *[a]

Hydrocarbon fuels can be produced from a wide range of carbonaceous materials, including biomass and waste plastics, through the Fischer–Tropsch (FT) process. As sustainable aviation fuel (SAF) becomes increasingly important, selective production of a jet fuel fraction from FT wax is required; however, this has not yet been achieved. In this study, hydrocracking of *n*-heptadecane (*n*-C17) as a model diesel fuel fraction of FT wax was estimated to obtain a jet fuel fraction selectively using Hβ-zeolite-Al_2O_3 composite-supported Pt catalysts. The Hβ-zeolite (25 wt%, SiO_2/Al_2O_3 = 100)-Al_2O_3 (60 wt%)-binder (alumina-sol, 15 wt% as Al_2O_3) composite-supported Pt (0.5 wt%) catalyst (0.5Pt/β(100)60A) was tested for hydrocracking of *n*-heptadecane using a fixed-bed flow reactor under the following conditions: 0.5 MPa H_2 pressure, H_2 300 mL min^{-1}, WHSV 2.3 h^{-1} and 2 g catalyst weight. After hydrocracking of *n*-C17 to form gaseous hydrocarbons at 300 °C without pre-reduction of 0.5Pt/β(100)60A, the reaction was performed at 250 °C. A conversion of 97% and a selectivity of 79% for the C8–C14 fraction of the jet fuel range were achieved. The sum of the selectivity for the C7 and C8 fractions was higher than 50%. To confirm reproducibility, when the hydrocracking of *n*-C17 using the catalyst pre-reduced at 270 °C was performed at 300–304 °C, a conversion of 93% and a selectivity of 55% for C8–C14 were achieved at 302 °C, with high selectivity for C8 and C9, although significant amounts of gaseous products were observed simultaneously. Finally, when the hydrocracking of *n*-C17 using a catalyst pre-reduced at 310 °C was performed at 300–308 °C, a conversion of 99% and a selectivity of 63% for C8–C14 were achieved at 308 °C, and the selectivity for gaseous products reduced to 16%. However, the high selectivity for C8 and C9 was lost, and the same amount of each fraction of C8–C12 was simultaneously observed. It was suggested that the high selectivity of the β-zeolite-containing catalyst for the C8 and C9 fractions could be attributed to C–H bond activation of the carbon at position 9 of *n*-C17 on reduced Pt within the micropores of β-zeolite.

Received 4th April 2025
Accepted 20th June 2025

DOI: 10.1039/d5ra02332g

rsc.li/rsc-advances

1. Introduction

As hydrocarbon fuels have high energy density, they can be utilized in internal combustion engines; however, given current environmental concerns, they should be obtained from carbon-neutral systems. Fischer–Tropsch synthesis (FTS) can be used to generate hydrocarbon fuels from synthesis gas derived from carbon-neutral biomass, waste plastics or carbon dioxide. On the other hand, since FTS has low product selectivity and produces a wide range of hydrocarbons, from gas to wax, heavier long-chained hydrocarbon fractions produced by FTS must be converted into gasoline, jet fuel, kerosene, or diesel oil *via* catalytic cracking or hydrocracking.[1,2] However, the selective conversion of long-chained hydrocarbons into desirable liquid fuels is very difficult. Therefore, the development of catalysts with high product selectivity is required.

Since liquid phase jet fuel is likely to be used well in the future, the production of jet fuel from hydrocracking of FT products is likely to be one of the most important catalytic processes.[3–9] For example, Pt/SiO_2–Al_2O_3,[3] Pt/H-beta,[4–6] Pt/H-ZSM-5,[4–6] Pt/H-mordenite,[4–6] and Pt/Al-mesoporous silica[9] have been used as catalysts in flow-type[4,7] and batch-type[5,6] reactors. Pt/H-beta showed good performance[4–6] probably because of the relatively high number of accessible acid sites;[4] the jet fuel was generated with a maximum yield of 22% at 250 °C and 1.5 MPa.[5] The product distribution shifted to compounds with lower

[a]*Division of Chemistry for Materials, Graduate School of Engineering, Mie University, 1577 Kurima Machiya-Cho, Tsu City, Mie Prefecture, 514-8507, Japan. E-mail: ishihara@chem.mie-u.ac.jp*

[b]*Zeolite Group, Institute of Inorganic Materials, Nanyou Office, Tosoh Corporation, 4560 Kaisei-Cho, Shunan City, Yamaguchi Prefecture 746-8501, Japan*

† Electronic supplementary information (ESI) available. See DOI: https://doi.org/10.1039/d5ra02332g

molecular weight when the temperature was increased or the pressure was decreased.[9] When FT wax containing 7% lighter fraction (<170 °C), 46% jet fuel (170–300 °C) and 47% heavier fraction (>300 °C) components, was converted at 330 °C and 5 MPa on Pt/Al-mesoporous silica with a SiO_2/Al_2O_3 ratio of 20, liquid products containing 18% gasoline, 63% jet fuel, and 19% heavier fraction were obtained.[9] As feed oil includes a larger amount of jet fuel fraction at the initial stage, in this case, 29% of the heavy fraction was hydrocracked, but only 16% jet fuel was achieved. These results indicate that the selectivity would not be sufficient to meet the high demand for jet fuel.

The ASTM D-1655 sets out civil standards for Jet A, Jet A-1 and Jet B fuels, which correspond to no. 1, no. 2 and no. 3 in JIS K 2209, respectively. Jet A and Jet A-1 are primarily composed of the kerosene fraction, while Jet B, which can be used in colder environments, includes not only kerosene but also significant amounts of the gasoline fraction. As hydrocarbons with carbon numbers from C8 to C16 could cover these standards, research groups aim to obtain this range of hydrocarbons from larger materials. In order to develop catalysts with increased product selectivity, understanding the reaction mechanisms of hydrocracking of FT wax or straight-chained long hydrocarbons on catalysts is necessary; to this end, model compounds consisting of long hydrocarbons have been used in many studies. Among them, *n*-hexadecane is one of most commonly used compounds,[10–29] and *n*-heptadecane,[2,21] *n*-octadecane,[30] bio-hydrogenated alkanes,[31,32] polymers[33,34] and biomass[35–57] have also been used; however, the jet fuel yield was not sufficient. In *n*-hexadecane hydrocracking, supported Pt and Pd catalysts have usually been used, with Pt and Pd loadings of 0.5–1 wt%. To date, MCM-41,[10] β-zeolite,[11] dealuminated HY-zeolite,[12] SBA-15/β-zeolite composite,[13] ZSM-22,[14] and heteropolymolybdate/MCM-41 composite[16] have been used as supports. Pt catalysts supported on dealuminated HY-zeolite[12] and SBA-15/β-zeolite composite[13] were used to generate jet fuel fractions of 51% using higher temperature and pressure.

We previously attempted to obtain jet fuel range oil selectively through hydrocracking of *n*-C17. When 0.5 wt% Pt was supported on a composite composed of 50 wt% HY-zeolite (SiO_2/Al_2O_3 = 100) and 50 wt% Al_2O_3, the C8–C14 range of products was obtained with a selectivity of 74% and 99% conversion at 295 °C and 0.5 MPa.[2] This result was very close to the ideal jet fuel yield (C8–C14) of 75% by weight, which is calculated on the basis of the assumptions discussed below.

When a carbocation is generated at the 2- to 16-positions in *n*-C17 and undergoes β-scission with the same probability, hydrocarbon products are formed with the same mole number for each fraction from C3 to C14. When a similar calculation is applied for *n*-C16, the maximum yield of C8–C13 is 72%, which differs significantly from reported results using *n*-C16. As the composite support included only 50 wt% zeolite in our study, the acidity of the zeolite was reduced, which led to the inhibition of over-cracking. In order to increase the yield of jet fuel (the middle range of hydrocarbons), this concept seems to be very important. Further, the size of the super cage of Y-zeolite was appropriate to retain longer-chained hydrocarbons inside before cracking; this would result in each carbocation being generated in *n*-C17 and undergoing β-scission with the same probability. On the other hand, the use of ZSM-5, with a small micropore size, resulted in over-cracking to generate gaseous products and C5–C7 fractions.[2]

In the course of our study, we were interested in hydrocracking using β-zeolite, which has a middle range of micropores between those of Y-zeolite and ZSM-5. The aim of this study was to selectively obtain jet fuel range products through hydrocracking using Pt-loaded β-zeolite-containing hierarchical catalysts, which were prepared with mesoporous Al_2O_3 by a kneading method. *n*-Heptadecane was also used as a model raw liquid from the hydrotreatment of fat or cracking of FT wax. The results were compared with those obtained using Y-zeolite-containing catalysts.

2. Experimental

2.1 Preparation of Pt/β-zeolite-Al_2O_3 catalysts

A composite support was prepared by the kneading method with Hβ-zeolite (SiO_2/Al_2O_3 = 100, HSZ-960HOA, Tosoh), Al_2O_3 (270 m^2 g^{-1}, Japan Ketjen) and alumina-sol (cataloid AP-1, JGC Catalyst Chemical). The content of β-zeolite, Al_2O_3 and binder alumina-sol was 50 : 35 : 15 or 25 : 60 : 15 by weight after calcination at 500 °C. After kneading, the clay-like material was pelletized and calcined. The resulting support was crushed and sieved to give 1 : 1 particles with 600–355 μm and 355–125 μm. The composite supports were named as β(100)35A and β(100)60A, where β indicates the type of zeolite, the number in a parenthesis indicates the SiO_2/Al_2O_3 ratio, and 35A or 60A indicates the 35 wt% or 60 wt% content of commercial Al_2O_3, respectively. Hydrogen hexachloroplatinate(IV) hexahydrate ($H_2PtCl_6 \cdot 6H_2O$, Fuji Film Wako Pure Chemical Industry Co., Ltd) was used to load 0.5 wt% of Pt on the support by the standard impregnation method. The catalyst was named Pt/composite support.

2.2 Characterization of Pt/β-zeolite-Al_2O_3 catalysts

X-ray diffraction (XRD), N_2 adsorption/desorption, ammonia-temperature programmed desorption (NH_3-TPD), transmission electron microscope (TEM), and thermogravimetry-differential thermal analysis (TG-DTA) were conducted to characterize the catalysts. Detailed methods and conditions were described elsewhere.[2]

An Ultima IV X-ray diffractometer was used (Rigaku Corporation). Fig. S1† shows the XRD patterns of 0.5Pt/β(100)35A and 0.5Pt/β(100)60A catalysts before and after the reaction. Only β-zeolite and γ-alumina were observed; signals derived from Pt were not detected, suggesting that the Pt was distributed throughout the catalysts.

BELPREP-vacII (Japan Bell Corporation) was used for pretreatment of the catalyst and a BELSORP-mini (Japan Bell Co., Ltd) was used for N_2 adsorption/desorption measurements. Table S1† shows the N_2 adsorption/desorption measurement results for 0.5Pt/β(100)35A and 0.5Pt/β(100)60A before and after the reaction. The differences between pore properties were very small, suggesting that the structures of the catalysts are almost identical.

To measure NH_3-TPD, NH_3 adsorbed at 100 °C on the catalyst was desorbed in the range of 100 °C to 650 °C under a He stream. NH_3 was detected by gas chromatography (GC) with a thermal conductivity detector (TCD) (GC-8A) under the conditions of INJ/IT 170 °C, COL 140 °C, ATTN 16, current 100 mA and column flow 30 cm^3 min^{-1}. Fig. S2 and Table S2† show the results of NH_3-TPD. Curve fitting was performed for NH_3-TPD of 0.5Pt/β(100)35A and 0.5Pt/β(100)60A, from which three sets of weak, strong, and very strong acid sites were estimated. Weak acid sites could be assigned to physical adsorption of NH_3, strong acid sites could be assigned to adsorption on zeolite, and very strong acid sites could be assigned to adsorption on Al_2O_3. It is thought that the very strong acid sites, whose content increased with increasing the amount of Al_2O_3, did not take part in the catalytic reaction at around 300 °C because their high reactivity would lead to deactivation during the early stages of the reaction. It was also concluded that weak acid sites, the amounts of which were very similar for 0.5Pt/β(100)35A and 0.5Pt/β(100)60A, were also not involved in the catalytic reaction. Strong acid sites, the number of which increased with increasing amounts of β-zeolite, could be involved in the catalytic reaction around 300 °C; therefore, the hydrocracking ability of 0.5Pt/β(100)35A was much higher than that of 0.5Pt/β(100)60A, as shown below. A zeolite with a SiO_2/Al_2O_3 ratio of 100 contains 3.3×10^{-4} mol per g Al. As the zeolite contents in 0.5Pt/β(100)35A and 0.5Pt/β(100)60A are 50% and 25%, respectively, the amounts of Al derived from zeolite are 1.6×10^{-4} and 0.82×10^{-4}, respectively. Values of strong acid sites for these catalysts were 4.1×10^{-4} and 2.4×10^{-4} mol g^{-1} as shown in Table S2,† which were much higher than the values calculated for the amounts of Al derived from β-zeolite, suggesting that physical adsorption of NH_3 on zeolite and Al_2O_3 would be included and that there might be the incorporation of Al species into the zeolite skeletal structure, which may increase the amount of strong acid sites.

TEM observations were performed using a JEM-1011 (Japan Electronics Co., Ltd) instrument. Fig. S3† shows TEM images of 0.5Pt/β(100)35A and 0.5Pt/β(100)60A catalysts before and after the reaction. In both catalyst systems, zeolite crystals with 500 nm were dispersed in the thin layer of Al_2O_3 and no significant difference was observed by TEM analysis before and after the reaction.

2.3 Hydrocracking of *n*-heptadecane using Pt/β-zeolite-Al_2O_3 catalysts

A stainless-steel fixed-bed flow reactor (ID 8 mm; OD 10 mm) was used for the hydrocracking of *n*-heptadecane. The reaction was performed for 2 hours at the same temperature; the liquid product obtained during the first hour was discarded and the product obtained during the second hour was collected and analyzed by gas chromatography with an FID detector (GC-FID). The catalyst (2 g; 600–355 μm (70 wt%) and 355–125 μm (30 wt%)) was reduced at 300 °C (H_2 30 mL min^{-1}) for 3 h, then hydrocracking was performed in the temperature range of 250–310 °C (H_2 pressure 0.5 MPa, H_2 flow rate 300 mL min^{-1}, weight hourly space velocity (WHSV): 2.3 h^{-1}). The gas and liquid products were separated in the gas–liquid separator and were analyzed separately by GC-FID (GC-2014 (Shimadzu Corp.) for gas product, GC-2010 (Shimadzu Corp.) for liquid products). No C1 and C2 products were formed. Detailed conditions of the GC analysis are described elsewhere.[2]

After the reaction, thermogravimetry-differential thermal analysis (TG-DTA; DTG-60AH, Shimadzu) was performed by heating the used catalysts to 600 °C under an air atmosphere to estimate the amount of coke deposited on the used catalysts; the results are summarized in Table S3.† As shown in Table S3,† coke formation was very low in this reaction at temperatures of around 300 °C under the given hydrogen pressure.

3. Results and discussion

3.1 Reaction profiles of 0.5Pt/β(100)60A and 0.5Pt/β(100)35A

As a preliminary experiment, *n*-heptadecane (*n*-C17) was decomposed on 0.5Pt/β(100)60A without pre-reduction under 0.5 MPa of hydrogen pressure at 300 °C. The conversion of *n*-C17 reached 100% and most of the products were gases. In order to obtain the jet fuel fraction, the temperature was decreased to 250 °C. The result (Fig. 1) showed that the conversion of *n*-C17 was 97% while the selectivity for the C8–C14 fraction reached 79%. Further, the selectivity for C8 and C9 fractions was more than 50%. We previously reported that 0.5Pt/Y(100)35A gave the C8–C14 fraction with 74% selectivity, wherein the selectivity for C8 and C9 was not so high, and that the products with each carbon number were obtained with similar selectivity.[2] Therefore, this suggests that the mechanism of hydrocracking of *n*-C17 might be different.

To establish the reproducibility, 0.5Pt/β(100)60A pre-reduced at 300 °C was used by dividing the reaction into four runs, with the temperature of the reactor reduced to 25 °C between runs. When the first reaction run was performed in the range of 250–260 °C for 10 hours, the maximum conversion was 14% at 260 °C and only isomers of C17 were obtained. When the second run was started at 270 °C, almost no hydrocracking occurred; thus, the reaction was performed in the range of 300–304 °C. The

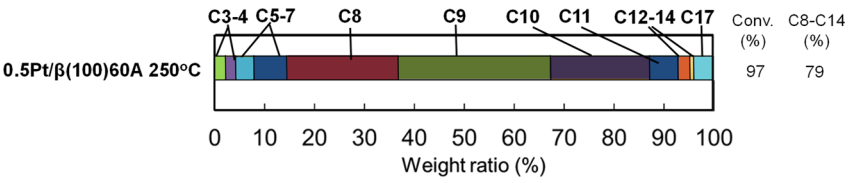

Fig. 1 Carbon number distribution of products in hydrocracking of *n*-heptadecane using 0.5Pt/β(100)60A without pre-reduction H_2 pressure 0.5 MPa, gas flow rate 300 cm^3 min^{-1}, WHSV 2.3 h^{-1}, catalyst 2.0 g.

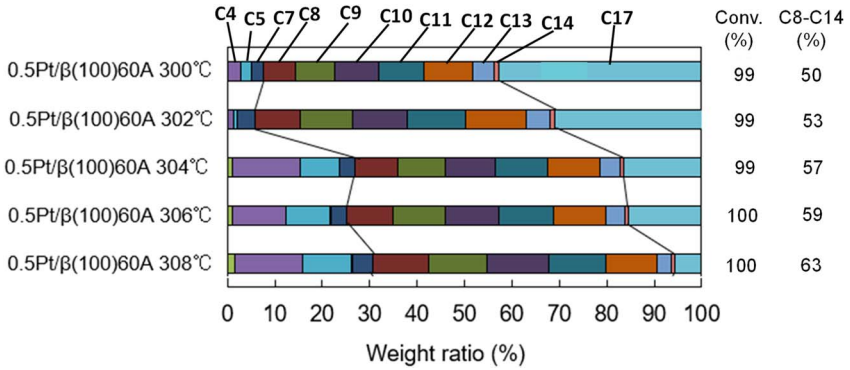

Fig. 2 Carbon number distribution of products in the second hydrocracking run of *n*-heptadecane using pre-reduced 0.5Pt/β(100)60A. Transfer order in reaction temp.: 270 → 300 → 304 → 303 → 302 → 301 °C. H_2 pressure 0.5 MPa, gas flow rate 300 cm^3 min^{-1}, WHSV 2.3 h^{-1}, catalyst 2.0 g.

order of temperature examined was: 300 °C →304 °C →303 °C →302 °C →301 °C. The conversion reached 100% at 304 °C and then the temperature was decreased. The detailed reaction profiles are shown in Fig. 2. Although the amount of gaseous products increased and the selectivity for C8–C14 fraction was distributed in the range of 39–55%, less than that shown in Fig. 1, high selectivity for C8 and C9 was also observed. In the third run, the reaction temperature was increased from 295 °C to 300 °C and the conversion increased from 85% to 100%. However, the selectivity for C8–C14 was less than 27% and isomerization occurred with a selectivity of more than 50% at each temperature. Therefore, the hydrocracking was started at 310 °C in the fourth run. The results are shown in Fig. 3. After it was confirmed that the conversion of *n*-C17 reached 100% and that significant amounts of gaseous products were observed at 310 °C, the reaction temperature was decreased by 2 °C to 300 °C. The conversions were 99–100% even when the temperature was reduced from 308 °C to 300 °C while the selectivity for the C8–C14 fraction decreased from 63% to 50%. In the fourth run, high yields of C8–C14 were achieved by tuning the temperature while the high selectivity for C8 and C9 disappeared and products with C8–C12 were obtained equally, indicating that highly active sites giving C8 and C9 selectively are deactivated, probably because the reactor was cooled to 25 °C between runs and coke deposition might occur at the highly active sites.

When the content of β-zeolite was increased in 0.5Pt/β(100)35A, the conversion increased significantly. The results are shown in Fig. 4. The reaction was started at 250 °C and the conversion was 57% at 255 °C. However, the conversion reached 100% at 260 °C and only gaseous products and the C5 fraction were selectively obtained, and no C8–C14 fraction was observed. When the temperature was decreased to 245 °C and 250 °C, high conversions of 80% and 96% were maintained while the major products were the C17 isomers. Therefore, fine tuning of temperature was performed; the results are shown in Fig. 5. After the reaction was started at 260 °C and 100% of conversion and the formation of gaseous products as a major component were confirmed, the reaction was traced in the order of 250 °C → 251 °C → 252 °C → 253 °C → 254 °C. The conversion increased from 92% to 95%, the selectivity for C17 isomers or C8–C14 fractions decreased, and the selectivity for gaseous products increased. C17 isomers were major products at 250–252 °C while gaseous products were major products at 253 °C and 254 °C. Therefore, the C8–C14 fraction could not be

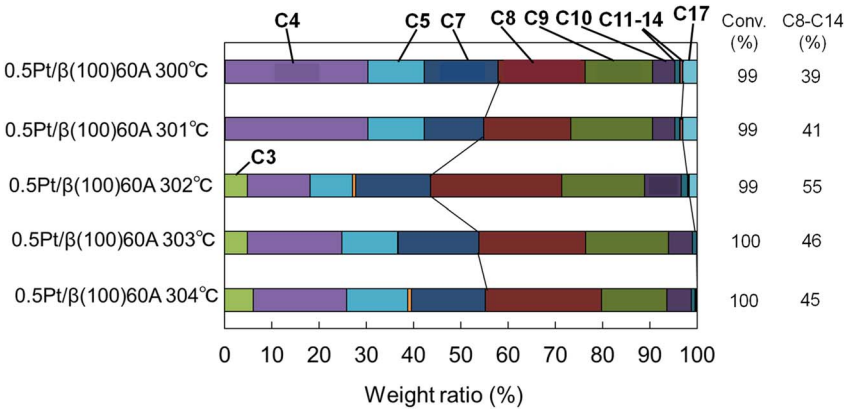

Fig. 3 Carbon number distribution of products in the fourth hydrocracking run of *n*-heptadecane using pre-reduced 0.5Pt/β(100)60A. Transfer order in reaction temp.: 310 → 308 → 306 → 304 → 302 → 300 °C. H_2 pressure 0.5 MPa, gas flow rate 300 cm^3 min^{-1}, WHSV 2.3 h^{-1}, catalyst 2.0 g.

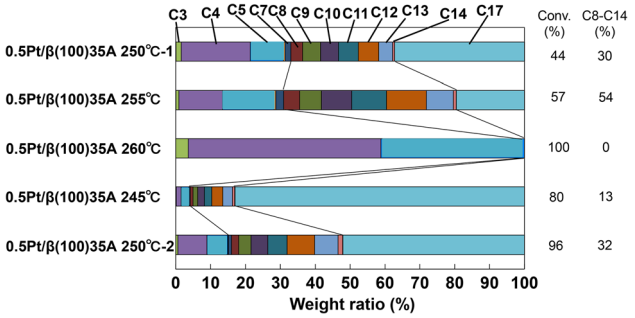

Fig. 4 Carbon number distribution of products in hydrocracking of *n*-heptadecane using pre-reduced 0.5Pt/β(100)35A. Transfer order in reaction temp.: 250 → 255 → 260 → 245 → 250 °C. H_2 pressure 0.5 MPa, gas flow rate 300 cm^3 min^{-1}, WHSV 2.3 h^{-1}, catalyst 2.0 g.

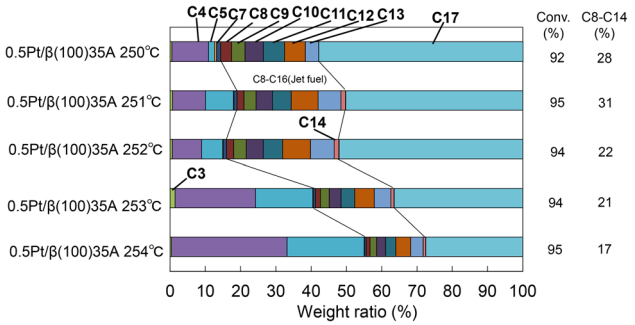

Fig. 5 Carbon number distribution of products in hydrocracking of *n*-heptadecane using pre-reduced 0.5Pt/β(100)35A. Transfer order in reaction temp.: 260 → 250 → 251 → 252 → 253 → 254 °C. H_2 pressure 0.5 MPa, gas flow rate 300 cm^3 min^{-1}, WHSV 2.3 h^{-1}, catalyst 2.0 g.

obtained as major products, indicating that the high content of β-zeolite renders the reaction difficult to control due to the presence of larger amounts of highly active sites.

3.2 Change in reaction mechanisms using 0.5Pt/β(100)60A

Fig. 6 shows the probable reaction mechanism for the selective production of C8 and C9 fractions on 0.5Pt/β(100)60A in the second run. In order to obtain C8 and C9 fractions selectively, a carbenium ion should be formed at the C8 or C10 position and a double bond should be formed between the C8 and C9 positions. The formation of the double bond could occur on Pt. The bending angle vibration of carbon–carbon bonds around the C9 position would be the most stable among those of all carbons in *n*-C17 because the vibration of these bonds does not bring about the rotation of the *n*-C17 molecule due to the bilateral symmetry at the C9 position. It is assumed that the possibility of this vibration could be high. The possibility that a hydrogen at the C9 position could approach the Pt species and interact with it would be the highest among the possibilities of hydrogens in a *n*-C17 molecule. Thus, the C–H bond activation at the C9 position occurs on Pt active species for these reasons, followed by dehydrogenation to form an olefin. The olefin interacts with a nearby acid site on the zeolite to form a carbenium ion at the

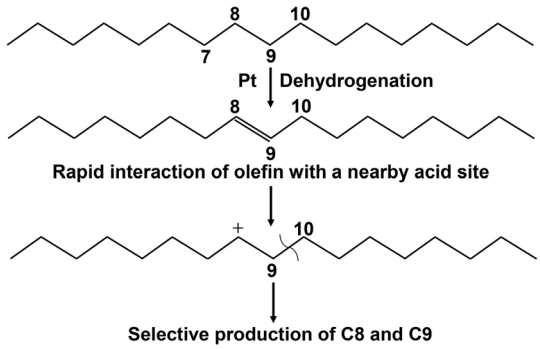

Fig. 6 Reaction mechanism for selective production of C8 and C9 fractions on 0.5Pt/β(100)60A in the second run.

C8 position because this carbenium has a less bulky alkyl chain with seven carbons. Subsequent β-scission at the C9–C10 bond would produce C9 and C8 hydrocarbons selectively.

Fig. 7 shows the hypothetical reaction routes on 0.5Pt/β(100)60A at 303 °C in the second run where C3, C4, C5 C7, C8, C9 and C10 fractions appeared. According to these routes, secondary carbenium ions are formed at the C8, C6, C4 and C2 positions, which subsequently undergo β-scission at the longer alkyl chains, suggesting that the longer alkyl chains could be cleaved more easily because these would be subjected to a heavier load. These results suggest that the secondary carbenium ion at the C8 position would interact with hydrogen at C6, C4 and C2, probably because such interactions form 4-, 6-, and 8-membered rings through the carbenium ion and each hydrogen atom, respectively, and the interaction through the 6-membered ring would be most probable.

Fig. 8 shows the reaction mechanism on 0.5Pt/β(100)60A in the fourth run. This mechanism can use the assumptions made for 0.5Pt/Y(100)35A,[2] where secondary carbenium ions are formed at positions C2 to C16 equally, aliphatic hydrocarbons from C3 to C14 are formed, C1 and C2 fractions are not formed, and β-scission proceeds with the same probability. According to these assumptions, the jet fuel fraction from C8 to C14 would be generated in 75% yield, which is consistent with the observed jet fuel yield of 73%, which indicates that the mechanism stated above would give the most probable routes. From the results of carbon number distribution in jet fuel fraction for the fourth run of 0.5Pt/β(100)60A shown in Fig. 3, it seems that the

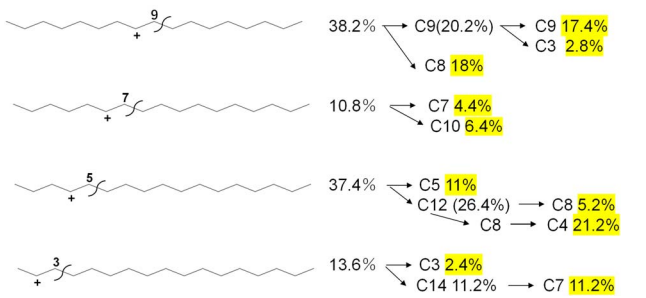

Fig. 7 Hypothetical reaction routes on 0.5Pt/β(100)60A at 303 °C in the second run.

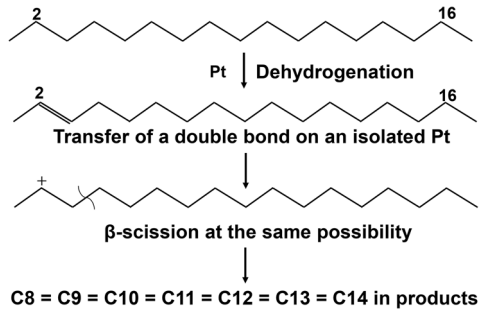

Fig. 8 Reaction mechanism on 0.5Pt/β(100)60A in the fourth run.

hydrocracking of *n*-C17 proceeded by a mechanism similar to that suggested for 0.5Pt/Y(100)35A.

Catalyst 0.5Pt/β(100)60A contains 2.6×10^{-5} mol per g Pt and 8.2×10^{-5} mol per g Al in β(100) and the Al/Pt ratio was 3.2. To obtain the higher selectivity for C8 and C9, the dehydrogenation at the C9 position on Pt and the interaction between the generated olefin and a nearby acid site must proceed immediately within the micropores of the β-zeolite. It seems that such selective production of C8 and C9 shown in the second run of 0.5Pt/β(100)60A (Fig. 2) proceeded at highly active sites where Pt and the acid sites are in close proximity. However, the high selectivity for C8 and C9 was lost in fourth run of 0.5Pt/β(100)60A (Fig. 3). As β-zeolite content was 25% and Pt is loaded on not only zeolite but also Al_2O_3, the amount of Pt loaded on the inside of the micropore in the β-zeolite would be significantly lower. Further, highly active sites where Pt and the acid site are in close proximity may be much fewer. Such active sites where Pt species and the acid sites co-exist within the micropores of the β-zeolite may be deactivated during the repeated runs because the catalyst is held at 25 °C for a long time between runs and olefins near the Pt species could be cyclized to form aromatic species and coke-like material.

Recently, hydrocracking of long-chained hydrocarbons producing jet fuel has also been reported.[58–61] It was shown that polyolefin hydrocracking using Ru/Y-zeolite catalysts was promoted when both metal and Brønsted acid sites are present and that the distance between metal and acid sites could determine this effect.[58] The distance between the metal and acid sites is also important in our hydrocracking of *n*-C17 using 0.5Pt/β(100)60A; the closer the olefins on metal sites are to the acid sites, the more easily the former interacts with the latter, leading to the higher selectivity for C8 and C9 production. In the hydrocracking of *n*-C16 using Pt/SAPO-11, the 37% yield of jet fuel was higher than that using Pt/HUSY, probably because of the weaker acidity of SAPO-11 than that of HUSY.[59] This result suggests that the acid site density is one of the most important factors determining jet fuel yield. While β(100) afforded an appropriate acid density in this study, more appropriate acid densities on the zeolite could be achieved by controlling its SiO_2/Al_2O_3 ratio and structure, such as in terms of pore size. This also suggests that a more appropriate active metal density within a zeolite could be important and that the best mix of acid and metal sites could give the highest selectivity for the jet fuel fraction.

4. Conclusions

Hydrocracking of FT wax or biomass-derived oils, such as fat, is one of the most promising methods for producing the jet fuel fraction of C8–C16. In the present study, *n*-C17 hydrocracking was performed using β-zeolite-Al_2O_3 composite-supported Pt catalysts in a fixed-bed reactor under the conditions of H_2 0.5 MPa, 300 mL min^{-1}, WHSV 2.3 h^{-1}, and catalyst weight 2 g. When 0.5Pt/β(100)60A was used (containing 0.5 wt% Pt, 25 wt% β-zeolite with $SiO_2/Al_2O_3 = 100$, 60 wt% of γ-Al_2O_3 and 15 wt% binder), initially at 300 °C and then at 250 °C, the jet fuel fraction of C8–C14 was obtained with 79% selectivity and 97% conversion. In this run, the selectivity for the C8 and C9 fractions was very high. To obtain reproducibly high selectivity for C8 and C9 fractions, the reaction of *n*-C17 was repeated under the same conditions after 0.5Pt/β(100)60A was pre-reduced at 300 °C. High selectivity for the C8 and C9 fractions was observed in the second run but was lost on the fourth run. The reasons for the high selectivity was discussed and the importance of the best mix of both acid and metal site densities within the zeolite micropore was suggested to lead to selective jet fuel production in the hydrocracking of long-chained hydrocarbons.

Data availability

The data supporting this article have been included as part of the ESI.†

Author contributions

Kosuke Murata: investigation, formal analysis, writing – original draft, and visualization. Yugo Nishiura: investigation, formal analysis, and writing – original draft. Shunma Mitsuoka: investigation, formal analysis, and writing – original draft. Mio Horibe: investigation, formal analysis, and writing – original draft. Tadanori Hashimoto: visualization and software. Ning Chen: conceptualization. Yuki Jonoo: resources. Sho Kawabe: project administration. Keita Nakao: funding acquisition. Atsushi Ishihara: supervision, methodology, data curation, and writing – review & editing.

Conflicts of interest

There are no conflicts of interest to declare.

Acknowledgements

The authors thank Mr Doi for his helpful work.

References

1 A. Ishihara, Preparation and reactivity of hierarchical catalysts in catalytic cracking, *Fuel Process. Technol.*, 2019, **194**, 106116, DOI: 10.1016/j.fuproc.2019.05.039.
2 S. Mitsuoka, K. Murata, T. Hashimoto, N. Chen, Y. Jonoo, S. Kawabe, K. Nakao and A. Ishihara, Production of Sustainable Aviation Fuel by Hydrocracking of n-

Heptadecane Using Pt-Supported Y-Zeolite-Al_2O_3 Composite Catalysts, *ACS Omega*, 2024, **9**(3), 3669–3674, DOI: 10.1021/acsomega.3c07678.

3 F. Link, C. M. Halmenschlager, G. Chauhan and A. de Klerk, Wax Hydrocracking over Pt/SiO_2-Al_2O_3 at 2 MPa: Product Characterization and Its Implications for Catalysis, *Energy Fuels*, 2021, **35**(6), 5252–5263, DOI: 10.1021/acs.energyfuels.0c04400.

4 S. Tomasek, F. Lonyi, J. Valyon, A. Wollmann and J. Hancsok, Hydrocracking of Fischer-Tropsch Paraffin Mixtures over Strong Acid Bifunctional Catalysts to Engine Fuels, *ACS Omega*, 2020, **5**(41), 26413–26420, DOI: 10.1021/acsomega.0c02711.

5 T. Hanaoka, T. Miyazawa, K. Shimura and S. Hirata, Jet fuel synthesis from Fischer-Tropsch product under mild hydrocracking conditions using Pt-loaded catalysts, *Chem. Eng. J.*, 2015, **263**, 178–185, DOI: 10.1016/j.cej.2014.11.042.

6 T. Hanaoka, T. Miyazawa, K. Shimura and S. Hirata, Jet fuel synthesis in hydrocracking of Fischer-Tropsch product over Pt-loaded zeolite catalysts prepared using microemulsions, *Fuel Process. Technol.*, 2015, **129**, 136–146, DOI: 10.1016/j.fuproc.2014.09.011.

7 J. Fratczak, H. P. Carmona, Z. Tisler, J. M. H. Herrador and Z. Gholami, Hydrocracking of Heavy Fischer-Tropsch Wax Distillation Residues and Its Blends with Vacuum Gas Oil Using Phonolite-Based Catalysts, *Molecules*, 2021, **26**(23), 7172, DOI: 10.3390/molecules26237172.

8 M. I. Hosukoglu, M. Karakaya and A. K. Avci, Modeling and Simulation of Hydrocracking of Fischer-Tropsch Hydrocarbons in a Catalytic Microchannel Reactor, *Ind. Eng. Chem. Res.*, 2012, **51**(26), 8913–8921.

9 S. Vedachalam, P. Boahene and A. K. Dalai, Production of jet fuel by hydrorefining of Fischer-Tropsch wax over Pt/Al-TUD-1 bifunctional catalyst, *Fuel*, 2021, **300**, 121008, DOI: 10.1016/j.fuel.2021.121008.

10 D. E. Romero, M. Rigato and E. J. M. Hansen, Influence of the size, order and topology of mesopores in bifunctional Pd-containing acidic SBA-15 and M41S catalysts for n-hexadecane hydrocracking, *Fuel Process. Technol.*, 2022, **232**, 107259, DOI: 10.1016/j.fuproc.2022.107259.

11 S. S. Mabaleha, Secondary cracking suppression through Pt/H-BEA: n-Hexadecane hydrocracking, *Microporous Mesoporous Mater.*, 2022, **337**, 111902, DOI: 10.1016/j.micromeso.2022.111902.

12 Y. Li, C. Mu, G. Chu, Y. Wang, J. Xu, X. Guo, Y. Zhao, S. Wang and X. Ma, Maximizing jet fuel production from n-hexadecane hydrocracking over Pt-supported Y catalysts: Importance of ideal hydrocracking characteristics, *Fuel*, 2023, **346**, 128286, DOI: 10.1016/j.fuel.2023.128286.

13 K. Jaroszewska, M. Fedyna and J. Trawczyński, Hydroisomerization of long-chain n-alkanes over Pt/AlSBA-15+zeolite bimodal catalysts, *Appl. Catal., B*, 2019, **255**, 117756, DOI: 10.1016/j.apcatb.2019.117756.

14 Y. Li, J. Sun, J. Wei, C. Mu, Y. Zhao, S. Wang and X. Ma, Cascade hydrogenation of n-C16 to produce jet fuel over tandem catalysts of modified ZSM-22, *J. Ind. Eng. Chem.*, 2022, **111**, 88–97, DOI: 10.1016/j.jiec.2022.03.039.

15 M. Azkaar, Z. Vajglová, P. Mäki-Arvela, A. Aho, N. Kumar, H. Palonen, K. Eränen, M. Peurla, L. A. Kulikov, A. L. Maximov, C. Mondelli, J. Pérez-Ramírez and D. Y. Murzin, Hydrocracking of hexadecane to jet fuel components over hierarchical Ru-modified faujasite zeolite, *Fuel*, 2020, **278**, 118193, DOI: 10.1016/j.fuel.2020.118193.

16 J. Sun, Y. Li, C. Mu, J. Wei, Y. Zhao, X. Ma and S. Wang, Supported heteropolyacids catalysts for the selective hydrocracking and isomerization of n-C16 to produce jet fuel, *Appl. Catal., A*, 2020, **598**, 117556, DOI: 10.1016/j.apcata.2020.117556.

17 R. Brosius, P. J. Kooyman and J. C. Q. Fletcher, Selective Formation of Linear Alkanes from n-Hexadecane Primary Hydrocracking in Shape-Selective MFI Zeolites by Competitive Adsorption of Water, *ACS Catal.*, 2016, **6**, 7710–7715, DOI: 10.1021/acscatal.6b02223.

18 Y. K. Krisnandi, I. R. Saragi, R. Sihombing, R. Ekananda, I. P. Sari, B. E. Grith and J. V. Hanna, Synthesis and Characterization of Crystalline NaY-Zeolite from Belitung Kaolin as Catalyst for n-Hexadecane Cracking, *Crystals*, 2019, **9**, 404–417, DOI: 10.3390/cryst9080404.

19 X. Wang, Z. Yu, J. Sun, Q. Wei, H. Liu, W. Huang, L. Zhao, M. Si and Y. Zhou, Synthesis of Small Crystal Size Y Zeolite Catalysts with High Hydrocracking Performance on n-Hexadecane, *Energy Fuels*, 2022, **36**, 13817–13832, DOI: 10.1021/acs.energyfuels.2c02851.

20 J. Weitkamp, P. A. Jacobs and J. A. Martens, Isomerization and hydrocracking of C9 through C16 n-alkanes on Pt/HZSM-5 zeolite, *Appl. Catal.*, 1983, **8**, 123–141.

21 E. J. P. Feijen, J. A. Martens and P. A. Jacobs, Isomerization and hydrocracking of decane and heptadecane on cubic and hexagonal faujasite zeolites and their intergrowth structures, *Stud. Surf. Sci. Catal.*, 1996, **101**, 721–729, DOI: 10.1016/S0167-2991(96)80283-7.

22 V. Calemma, S. Peratello and C. Perego, Hydroisomerization and hydrocracking of long chain n-alkanes on Pt/amorphous SiO_2–Al_2O_3 catalyst, *Appl. Catal., A*, 2000, **190**, 207–218.

23 K.-C. Park and S.-K. Ihm, Comparison of Pt/zeolite catalysts for n-hexadecane hydroisomerization, *Appl. Catal., A*, 2000, **203**, 201–209.

24 I. Rossetti, C. Gambaro and V. Calemma, Hydrocracking of long chain linear paraffins, *Chem. Eng. J.*, 2009, **154**, 295–301.

25 J. Kang, W. Ma, R. A. Keogh, W. D. Shafer, G. Jacobs and B. H. Davis, Hydrocracking and hydroisomerization of n-hexadecane, noctacosane and Fischer–Tropsch wax over a Pt/SiO_2–Al_2O_3 catalyst, *Catal. Lett.*, 2012, **142**, 1295–1305.

26 F. Regali, M. Boutonnet and S. Jaras, Hydrocracking of n-hexadecane on noble metal/silica–alumina catalysts, *Catal. Today*, 2013, **214**, 12–18.

27 F. Regali, L. F. Liotta, A. M. Venezia, V. Montes, M. Boutonnet and S. Jaras, Effect of metal loading on activity, selectivity and deactivation behavior of Pd/silica–alumina catalysts in the hydroconversion of n-hexadecane, *Catal. Today*, 2014, **223**, 87–96.

28 P. Lanzafame, S. Perathoner, G. Centi, E. Heracleous, E. F. Iliopoulou, K. S. Triantafyllidis and A. A. Lappas, Effect of the structure and mesoporosity in Ni/Zeolite catalysts for n-hexadecane hydroisomerisation and hydrocracking, *ChemCatChem*, 2017, **9**, 1632–1640.

29 T. Kaka khel, P. Mäki-Arvela, M. Azkaar, Z. Vajglová, A. Aho, J. Hemming, M. Peurla, K. Eränen, N. Kumar and D. Y. Murzin, Hexadecane hydrocracking for production of jet fuels from renewable diesel over proton and metal modified H-Beta zeolites, *Mol. Catal.*, 2019, **476**, 110515, DOI: **10.1016/j.mcat.2019.110515**.

30 S. Bhattacharjee and C.-S. Tan, Production of Biojet Fuel from Octadecane and Derivatives of Castor Oil Using a Bifunctional Catalyst Ni–Pd@Al-MCF in a Pressurized CO_2–Hexane–Water Solvent, *Energy Fuels*, 2022, **36**, 3119–3133, DOI: **10.1021/acs.energyfuels.1c03881**.

31 T. Hengsawad, C. Srimingkwanchai, S. Butnark, D. E. Resasco and S. Jongpatiwut, Effect of Metal–Acid Balance on Hydroprocessed Renewable Jet Fuel Synthesis from Hydrocracking and Hydroisomerization of Biohydrogenated Diesel over Pt-Supported Catalysts, *Ind. Eng. Chem. Res.*, 2018, **57**, 1429–1440.

32 M. Lu, X. Liu, Y. Li, Y. Nie, X. Lu, D. Deng, Q. Xie and J. Ji, Hydrocracking of bio-alkanes over Pt/Al-MCM-41 mesoporous molecular sieves for bio- jet fuel production, *Mol. Catal.*, 2016, **8**(5), 053103/1–053103/12, DOI: **10.1063/1.4962561**.

33 T. Luo, W. Zhou, Y. Wang, H. Jiang, J. Wu, J. Hu, M. Wang, W. Wang, Q. Wang, Y. Hu, *et al.*, Integrating microwave pyrolysis and hydrotreating for converting low-density polyethylene into jet fuel, *Renew. Energy*, 2024, **236**, 121432.

34 L. Li, H. Luo, Z. Shao, H. Zhou, J. Lu, J. Chen, C. Huang, S. Zhang, X. Liu, L. Xia, J. Li, H. Wang and Y. Sun, Converting Plastic Wastes to Naphtha for Closing the Plastic Loop, *J. Am. Chem. Soc.*, 2023, **145**, 1847–1854, DOI: **10.1021/jacs.2c11407**.

35 A. Ishihara, N. Fukui, H. Nasu and T. Hashimoto, Hydrocracking of soybean oil using zeolite–alumina composite supported NiMo catalysts, *Fuel*, 2014, **134**, 611–617, DOI: **10.1016/j.fuel.2014.06.004**.

36 N. Chen, S. Gong, H. Shirai, T. Watanabe and E. W. Qian, Effects of Si/Al ratio and Pt loading on Pt/SAPO-11 catalysts in hydroconversion of Jatropha oil, *Appl. Catal., A*, 2013, **466**, 105–115, DOI: **10.1016/j.apcata.2013.06.034**.

37 Y. Shirasaki, H. Nasu, T. Hashimoto and A. Ishihara, Effects of types of zeolite and oxide and preparation methods on dehydrocyclization-cracking of soybean oil using hierarchical zeolite-oxide composite-supported Pt/NiMo sulfided catalysts, *Fuel Process. Technol.*, 2019, **194**, 106109, DOI: **10.1016/j.fuproc.2019.05.032**.

38 Y. Wu, X. Liu, J. Zhang, Y. Zhang, X. Li, H. Xia and F. Wang, Direct Production of Jet Fuel by Catalytic Hydrocracking of Glycerol Trioleate over a Ni/Mo Catalyst Supported on Nb_2O_5-ZrO_2, *Ind. Eng. Chem. Res.*, 2022, **61**(34), 12338–12348, DOI: **10.1021/acs.iecr.2c00731**.

39 M. C. Vasquez, E. E. Silva and E. F. Castillo, Hydrotreatment of vegetable oils: A review of the technologies and its developments for jet biofuel production, *Biomass Bioenergy*, 2017, **105**, 197–206, DOI: **10.1016/j.biombioe.2017.07.008**.

40 L. Chen, H. Li, J. Fu, C. Miao, P. Lv and Z. Yuan, Catalytic hydroprocessing of fatty acid methyl esters to renewable alkane fuels over Ni/HZSM-5 catalyst, *Catal. Today*, 2016, **259**(Part_2), 266–276, DOI: **10.1016/j.cattod.2015.08.023**.

41 D. Verma, B. S. Rana, R. Kumar, M. G. Sibi and A. K. Sinha, Diesel and aviation kerosene with desired aromatics from hydroprocessing of jatropha oil over hydrogenation catalysts supported on hierarchical mesoporous SAPO-11, *Appl. Catal., A*, 2015, **490**, 108–116, DOI: **10.1016/j.apcata.2014.11.007**.

42 S. H. Hassan, N. K. Attia, G. I. El Diwani, S. K. Amin, R. S. Ettouney and M. A. El-Rifai, Catalytic hydrocracking of jatropha oil over natural clay for bio- jet fuel production, *Sci. Rep.*, 2023, **13**(1), 13419, DOI: **10.1038/s41598-023-40500-2**.

43 T. Kimura, H. Imai, X. Li, K. Sakashita, S. Asaoka and S. S. Al-Khattaf, Hydroconversion of Triglycerides to Hydrocarbons Over Mo-Ni/γ-Al_2O_3 Catalyst Under Low Hydrogen Pressure, *Catal. Lett.*, 2013, **143**(11), 1175–1181.

44 C. Jia, C. Zhang, S. Xie, W. Zhang, Z. Wang and H. Lin, One-pot production of jet fuels from fatty acids and vegetable oils in biphasic tandem catalytic process, *Fuel*, 2021, **302**, 121060.

45 K. Zhang, X. Zhang and T. Tan, The production of bio- jet fuel from Botryococcus braunii liquid over a Ru/CeO catalyst, *RSC Adv.*, 2016, **6**(102), 99842–99850.

46 Y.-K. Chen, C.-H. Hsieh and W.-C. Wang, The production of renewable aviation fuel from waste cooking oil. Part II: Catalytic hydrocracking/isomerization of hydro-processed alkanes into jet fuel range products, *Renew. Energy*, 2020, **157**, 731–740.

47 Z. Eller, Z. Varga and J. Hancsok, Advanced production process of jet fuel components from technical grade coconut oil with special hydrocracking, *Fuel*, 2016, **182**, 713–720.

48 M. Y. Kim, J.-K. Kim, M.-E. Lee, S. Lee and M. Choi, Maximizing Biojet Fuel Production from Triglyceride: Importance of the Hydrocracking Catalyst and Separate Deoxygenation/Hydrocracking Steps, *ACS Catal.*, 2017, **7**(9), 6256–6267.

49 C. Ju, F. Wang, Y. Huang and Y. Fang, Selective extraction of neutral lipid from wet algae paste and subsequently hydroconversion into renewable jet fuel, *Renewable Energy*, 2018, **118**, 521–526, DOI: **10.1016/j.renene.2017.11.028**.

50 D. Verma, R. Kumar, B. S. Rana and A. K. Sinha, Aviation fuel production from lipids by a single-step route using hierarchical mesoporous zeolites, *Energy Environ. Sci.*, 2011, **4**(5), 1667–1671, DOI: **10.1039/c0ee00744g**.

51 C.-H. Lin and W.-C. Wang, Direct conversion of glyceride-based oil into renewable jet fuels, *Renewable Sustainable Energy Rev.*, 2020, **132**, 110109, DOI: **10.1016/j.rser.2020.110109**.

52 H. Jeong, H. B. Bathula, T. W. Kim, G. B. Han, J. H. Jang and B. Jeong, Superior Long-Term Stability of a Mesoporous Alumina-Supported Pt Catalyst in the Hydrodeoxygenation

of Palm Oil, *ACS Sustain. Chem. Eng.*, 2021, **9**, 1193–1202, DOI: **10.1021/acssuschemeng.0c06658**.

53 T. Li, J. Cheng, X. Zhang, J. Liu, R. Huang and J. Zhou, Jet range hydrocarbons converted from microalgal biodiesel over mesoporous zeolite-based catalysts, *Int. J. Hydrogen Energy*, 2018, **43**, 9988–9993, DOI: **10.1016/j.ijhydene.2018.04.078**.

54 T. Li, J. Cheng, R. Huang, W. Yang, J. Zhou and K. Cen, Hydrocracking of palm oil to jet biofuel over different zeolites, *Int. J. Hydrogen Energy*, 2016, **41**, 21883–21887, DOI: **10.1016/j.ijhydene.2016.09.013**.

55 J. Cheng, Z. Zhang, X. Zhang, J. Liu, J. Zhou and K. Cen, Sulfonated mesoporous Y zeolite with nickel to catalyze hydrocracking of microalgae biodiesel into jet fuel range hydrocarbons, *Int. J. Hydrogen Energy*, 2019, **4**, 1650–1658, DOI: **10.1016/j.ijhydene.2018.11.110**.

56 M. Zula, M. Grilc and B. Likozar, Hydrocracking, hydrogenation and hydro-deoxygenation of fatty acids, esters and glycerides: Mechanisms, kinetics and transport phenomena, *Chem. Eng. J.*, 2022, **444**, 136564, DOI: **10.1016/j.cej.2022.136564**.

57 A. Bjelić, M. Grilc, M. Huš and B. Likozar, Hydrogenation and hydrodeoxygenation of aromatic lignin monomers over Cu/C, Ni/C, Pd/C, Pt/C, Rh/C and Ru/C catalysts: Mechanisms, reaction micro-kinetic modelling and quantitative structure-activity relationships, *Chem. Eng. J.*, 2019, **359**, 305, DOI: **10.1016/j.cej.2018.11.107**.

58 T. Kwon, B. Ahn, K. H. Kang, W. Won and I. Ro, Unraveling the role of water in mechanism changes for economically viable catalytic plastic upcycling, *Nat. Commun.*, 2024, **15**(1), 10239, DOI: **10.1038/s41467-024-54495-5**.

59 C. Mu, J. Sun, C. Xie, J. Bao, X. Guo, H. Zhang, Y. Zhao, S. Wang and X. Ma, Shape selectivity of AEL channels for anomalously facilitating biojet fuel production from long-chain n-alkane hydrocracking, *ACS Catal.*, 2024, **14**(3), 1394–1404, DOI: **10.1021/acsami.2c11607**.

60 K. Kimura, T. Saika, T. Tsuchiya, H. Fujitsuka and T. Tago, Controlling catalytic activities for hydroisomerization and hydrocracking of long-chain alkanes using Pt-Mg-supported zeolite catalysts, *J. Jpn. Pet. Inst.*, 2024, **67**(5), 195–202, DOI: **10.1627/jpi.67.195**.

61 T. Fukumasa, Y. Kawatani, H. Masuda, I. Nakashita, R. Hashiguchi, M. Takemoto, S. Suganuma, E. Tsuji, T. Wakaihara and N. Katada, Shape selective cracking of polypropylene on an H-MFI type zeolite catalyst with recovery of cyclooctane solvent, *RSC Sustainability*, 2025, **3**(2), 890–903, DOI: **10.1039/d4su00484a**.